PAPER

Transparent PT-symmetric nonlinear networks

Physica Scripta

PAPER

Transparent PT-symmetric nonlinear networks

M E Akramov[1], J R Yusupov[2], M Ehrhardt[3], H Susanto[4] and D U Matrasulov[5,6]

[1] National University of Uzbekistan, Universitet Str. 4, 100174, Tashkent, Uzbekistan
[2] Kimyo International University in Tashkent, 156 Usman Nasyr Str., 100121, Tashkent, Uzbekistan
[3] Bergische Universität Wuppertal, Gaußstrasse 20, D-42119 Wuppertal, Germany
[4] Khalifa University, PO Box127788, Abu Dhabi, United Arab Emirates
[5] Turin Polytechnic University in Tashkent, 17 Niyazov Str., 100095, Tashkent, Uzbekistan
[6] Tashkent University of Architecture and Civil Engineering, Yangishahar Str. 9A, 100095 Tashkent, Uzbekistan

E-mail: j.yusupov@kiut.uz

RECEIVED
17 November 2024

REVISED
8 January 2025

ACCEPTED FOR PUBLICATION
21 February 2025

PUBLISHED
5 March 2025

Keywords: NNLS equation, metric graphs, transparent boundary conditions, potential approach, nonlinear optics

Abstract

We study reflectionless wave propagation in networks modeled by the nonlocal nonlinear Schrödinger equation on metric graphs, with transparent boundary conditions applied at the vertices. Using a 'potential approach' previously developed for the nonlinear Schrödinger equation, we derive transparent boundary conditions specific to the nonlocal nonlinear Schrödinger equation on metric graphs. These conditions prevent backscattering at the vertices, which is essential for reducing losses in signal, heat, and charge transfer in applications including optical fibers, optoelectronic networks, and low-dimensional materials.

1. Introduction

Nonlocal nonlinear Schrödinger (NNLS) equation attracted much attention since its pioneering study by Ablowitz and Muslimani published in the [1], where they showed integrability of the problem and obtained a soliton solution. An interesting feature of the soliton solution of the NNLS equation obtained by Ablowitz and Muslimany is caused by its nonlocality, i.e. the solution at a point x_1 depends on the solution at point $-x_1$. Another important feature is the fact that the NNLS equation is PT-symmetric. Later, various aspects of the NNLS equation were studied in a series of papers by Ablowitz and Muslimani [2–7] and other authors (see, e.g., [8–17]). In [15], the dynamical properties of periodic collisions of the Schrödinger equation with nonlocal nonlinearity are studied and the possible application of the model to soliton propagation in novel nonlocal nonlinear optical materials is discussed. In [16], the evolution characteristics of the periodic transmission of circularly symmetric multi-ring solitons in optical nonlocal materials based on the nonlinear Schrödinger equation are studied and the transmission expression of circularly symmetric multi-ring solitons has been derived. The [17] studies (based on the nonlocal nonlinear Schrödinger equation,) the nonlinear transmission characteristics of elliptical sine-Gaussian cross-phase beams in strongly nonlocal nonlinear media.

Besides nonlocality and PT symmetry, the NNLS equation has practical importance from the viewpoint of practical applications in nonlinear optics and some ferromagnetic structures. Here we consider the problem of transparent PT-symmetric nonlinear networks modeled in terms of the NNLS equation on metric graphs (see, e.g., [18, 19]) with a focus on transparent vertex boundary conditions. The latter means the boundary conditions that ensure the absence of backscattering at the graph vertex. To do this, we use the so-called 'potential approach', which was previously used to impose transparent vertex boundary conditions for the nonlinear Schrödinger (NLS) equation on metric graphs [20]. The idea of the approach is to consider the nonlinear term as a potential acting in the linear Schrödinger equation. Then the treatment of the NLS equation can be considered as the linear one, so that it can be treated as linear in the context of transparent boundary conditions [21].

The study of transparent boundary conditions (TBC) in networks is motivated by their relevance to several key technological applications, such as tunable soliton dynamics in branched optical fibers and optoelectronic

networks, as well as the control of quasiparticle transport in low-dimensional functional materials with branching structures. Over the last two decades, evolution equations on metric graphs have seen substantial interest across various fields [22–32]. In each of these cases, reducing signal, heat, and charge losses along the network requires carefully designed architectures.

The paper is organized as follows. In section 2 we briefly introduce soliton solutions and conserving quantities for NNLS equation on a line and recall the main steps of deriving the transparent boundary conditions. In section 3 we derive TBCs for the NNLS equation on metric graphs. section 4 demonstrates the verification of the obtained results by a numerical experiment. Finally, section 5 contains the concluding remarks.

2. TBC for the NNLS equation on a line

2.1. Soliton solutions of the NNLS equation

Consider the NNLS equation on a line

$$\mathrm{i}\partial_t q(x,\,t) + \partial_x^2 q(x,\,t) + 2q(x,\,t)q^*(-x,\,t)q(x,\,t) = 0, \tag{1}$$

where q^* represents the complex conjugate of q, and the self-induced potential, defined by $V(x,t) = 2\,q(x,t)\,q^*(-x,t)$, exhibits PT-symmetry, meaning $V(x,t) = V^*(-x,t)$. The nonlocality of equation (1) stems from the term $q^*(-x,t)$, indicating that the solution $q(x,t)$ at position x depends on information from the symmetric point $-x$. The NNLS equation supports several types of soliton solutions, such as breathing, rational, periodic, and more. For instance, a single soliton solution, derived via the inverse scattering method in [1], is given by:

$$q(x,\,t) = -\frac{2(\eta_1 + \bar{\eta}_1)\,e^{\mathrm{i}\bar{\theta}_1}\,e^{4\mathrm{i}\bar{\eta}_1^2 t}\,e^{-2\bar{\eta}_1 x}}{1 + e^{\mathrm{i}(\theta_1+\bar{\theta}_1)}\,e^{-4\mathrm{i}(\eta_1^2-\bar{\eta}_1^2)t}\,e^{-2(\eta_1+\bar{\eta}_1)x}}, \tag{2}$$

with real constants η_1, $\bar{\eta}_1$, θ_1, and $\bar{\theta}_1$. An important feature of this soliton solution (2) is the fact that it describes a wave that looks like a 'bird that flaps its wings but does not fly/move'.

A traveling soliton solution of equation (1) derived in [8] is written as

$$q(x,\,t) = \frac{\alpha_1\,e^{-\Delta/2}\,e^{(\bar{\xi}_{1R}-\xi_{1R})+\mathrm{i}(\bar{\xi}_{1I}-\xi_{1I})}}{2[\cosh(\chi_1)\cos(\chi_2) + \mathrm{i}\sinh(\chi_1)\sin(\chi_2)]}, \tag{3}$$

where

$$\chi_1 = (\xi_{1R} + \bar{\xi}_{1R} + \Delta_R)/2,$$

$$\chi_2 = (\xi_{1I} + \bar{\xi}_{1I} + \Delta_I)/2,$$

$$\xi_{1R} = -\mathcal{I}(k_1)(x + 2\mathfrak{R}(k_1)t), \quad \xi_{1I} = \mathfrak{R}(k_1)x - (\mathcal{I}(k_1)^2 - \mathfrak{R}(k_1)^2)t,$$

$$\bar{\xi}_{1R} = -\mathcal{I}(\bar{k}_1)(x + 2\mathfrak{R}(\bar{k}_1)t), \quad \bar{\xi}_{1I} = \mathfrak{R}(\bar{k}_1)x - (\mathfrak{R}(\bar{k}_1)^2 - \mathcal{I}(\bar{k}_1)^2)t,$$

$$\Delta_R = \log\left(\frac{|\alpha_1|^2|\beta_1|^2}{|k_1 + \bar{k}_1|^2}\right),$$

$$\Delta_I = -\frac{\mathrm{i}}{2}\log\left(\frac{\alpha_1\beta_1(k_1^* + \bar{k}_1^*)^2}{\alpha_1^*\beta_1^*(k_1 + \bar{k}_1)^2}\right),$$

$$\Delta = \log\left(-\frac{\alpha_1\beta_1}{(k_1 + \bar{k}_1)^2}\right),$$

with α_1, β_1, k_1 and $\bar{k}_1$ are arbitrary complex constants.

The integrability of the problem has been proven in [1], implying that the NNLS equation possesses infinitely many conservation laws. In particular, two key conserved quantities, the norm and the energy, were derived in [1] and are expressed as follows:

$$N(t) = \int_{-\infty}^{+\infty} q(x,\,t)\,q^*(-x,\,t)\,dx,$$

$$E(t) = \int_{-\infty}^{+\infty} [\partial_x q(x,\,t)\cdot\partial_x q^*(-x,\,t) + q^2(x,\,t)\cdot q^{*2}(-x,\,t)]\,dx. \tag{4}$$

Soliton solutions of equation (1), presented above, are derived under the assumption of decay conditions at infinity, i.e., $q(x,t) \to 0$ as $x \to \pm\infty$.

2.2. Transparent boundary conditions

Following [33], we briefly review the problem of transparent boundary conditions for the NNLS equation on a line, which is based on the so-called *potential approach* originally adopted for NLS equation in [34]. This method has proven effective in deriving TBCs for various nonlinear evolution equations, as shown in [33, 35, 36]. Using this approach, the NNLS equation can be formally reduced to the linear Schrödinger equation

$$\mathrm{i}\partial_t q(x,\,t) + \partial_x^2 q(x,\,t) + V(x,\,t)q(x,\,t) = 0, \tag{5}$$

with the potential $V(x,t) = 2q(x,t)q^*(-x,t)$. By introducing a new unknown

$$Q(x,\,t) = e^{-\mathrm{i}\mathcal{V}(x,t)}\, q(x,\,t), \tag{6}$$

with

$$\mathcal{V}(x,\,t) = \int_0^t V(x,\,s)\, ds, \tag{7}$$

the Schrödinger equation can be writen for $Q(x,t)$ as

$$\mathrm{i}\partial_t Q + \partial_x^2 Q + A\partial_x Q + BQ = 0, \tag{8}$$

where $A = 2\mathrm{i}\partial_x\mathcal{V}$ and $B = (\mathrm{i}\partial_x^2\mathcal{V} - (\partial_x\mathcal{V})^2)$. Next, based on proposition 2.1 and its proof in [34], one can rewrite equation (8) as (using the pseudo-differential operator calculus [37]):

$$(\partial_x + \mathrm{i}\Lambda^-)(\partial_x + \mathrm{i}\Lambda^+) = \partial_x^2 + \mathrm{i}(\Lambda^+ + \Lambda_-)\partial_x + \mathrm{iOp}(\partial_x\lambda^+) - \Lambda^+\Lambda^-, \tag{9}$$

where λ^+ represents the principal symbol of the operator Λ^+, and $\mathrm{Op}(p)$ denotes the operator associated with the symbol p by inverse Fourier transform. The, from equations (8) and (9) one obtains the following system

$$\begin{aligned} &\mathrm{i}(\Lambda^+ + \Lambda^-) = A,\\ &\mathrm{iOp}(\partial_x\lambda^+) - \Lambda^+\Lambda^- = \mathrm{i}\partial_t + B. \end{aligned} \tag{10}$$

This leads to the symbolic system of equations

$$\begin{aligned} &\mathrm{i}(\lambda^+ + \lambda^-) = a,\\ &\mathrm{i}\partial_x\lambda^+ - \sum_{\alpha=0}^{+\infty}\frac{(-1)^\alpha}{\alpha\,!}\partial_\tau^\alpha\lambda^-\partial_t^\alpha\lambda^+ = -\tau + b, \end{aligned} \tag{11}$$

where τ is the time covariable, $\mathrm{Op}(a) = A$ and $\mathrm{Op}(b) = B$, since the two functions A and B correspond to zero-order operators.

Then, the total symbol $\lambda^\pm$ is expressed as an asymptotic expansion in the inhomogeneous symbols as

$$\lambda^\pm \sim \sum_{j=0}^{+\infty}\lambda^\pm_{1/2-j/2}. \tag{12}$$

The upper relation of (11) and expansion (12) admits to determine the $1/2$-order terms:

$$\lambda^-_{1/2} = -\lambda^+_{1/2}, \qquad \lambda^+_{1/2} = \pm\sqrt{-\tau}, \tag{13}$$

where the associated operator of the symbol $\sqrt{\tau}$ is the half-order fractional derivative operator $e^{-i\frac{\pi}{4}}\partial_t^{1/2}$, and the choice $\lambda^+_{1/2} = \pm\sqrt{-\tau}$ corresponds to the Dirichlet-to-Neumann (DtN) operator. Now, for the zeroth-order terms we can write a system of equations as

$$\begin{aligned} &\lambda_0^- = -\lambda_0^+ - \mathrm{i}a,\\ &\mathrm{i}\partial_x\lambda^+_{1/2} - (\lambda_0^-\lambda^+_{1/2} + \lambda_0^+\lambda^-_{1/2}) = 0. \end{aligned} \tag{14}$$

Then, equation (14) with equation (13) leads to

$$\begin{aligned} &\lambda_0^+ = -\mathrm{i}\tfrac{a}{2} = \tfrac{1}{2}\partial_x\mathcal{V},\\ &\lambda_0^- = -\lambda_0^+ - \mathrm{i}a = \tfrac{1}{2}\partial_x\mathcal{V}. \end{aligned} \tag{15}$$

Since $\partial_t^\alpha\lambda^\pm_{-1/2} = \partial_\tau^\alpha\lambda_0^\pm = 0, \alpha\in N$, the terms of order $-1/2$ can also be calculated from

$$\begin{aligned} &\mathrm{i}(\lambda^+_{-1/2} + \lambda^-_{-1/2}) = 0,\\ &\mathrm{i}\partial_x\lambda_0^+ - (\lambda^-_{-1/2}\lambda^+_{1/2} + \lambda_0^+\lambda_0^- + \lambda^+_{-1/2}\lambda^-_{1/2}) = b, \end{aligned} \tag{16}$$

which results in

$$\lambda^\pm_{-1/2} = 0. \tag{17}$$

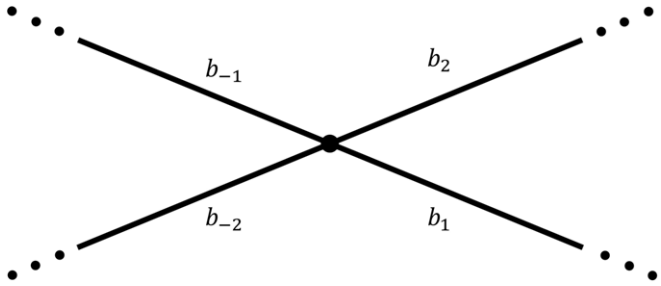

Figure 1. The simplest symmetric star graph with four bonds.

Continuing, one can obtain the next order terms as

$$\lambda_{-1}^{-} = -\lambda_{-1}^{+}, \quad \lambda_{-1}^{+} = \mathrm{i}\frac{\partial_x V}{4\tau}. \tag{18}$$

As a result, TBCs were derived up to the second-order approximation:

$$\partial_x q|_{x=-L} - e^{-\mathrm{i}\frac{\pi}{4}} e^{\mathrm{i}\mathcal{V}} \partial_t^{1/2}(e^{-\mathrm{i}\mathcal{V}} q)|_{x=-L} - \mathrm{i}\frac{\partial_x V}{4} e^{\mathrm{i}\mathcal{V}} I_t(e^{-\mathrm{i}\mathcal{V}} q)|_{x=-L} = 0, \tag{19a}$$

$$\partial_x q|_{x=L} + e^{-\mathrm{i}\frac{\pi}{4}} e^{\mathrm{i}\mathcal{V}} \partial_t^{1/2}(e^{-\mathrm{i}\mathcal{V}} q)|_{x=L} + \mathrm{i}\frac{\partial_x V}{4} e^{\mathrm{i}\mathcal{V}} I_t(e^{-\mathrm{i}\mathcal{V}} q)|_{x=L} = 0, \tag{19b}$$

where the half-order fractional time derivative operator, is defined as

$$(\partial_t^{1/2} f)(t) = \frac{1}{\sqrt{\pi}} \partial_t \int_0^t \frac{f(s)}{\sqrt{t-s}}\, ds, \tag{20}$$

and the operator $I_t(f)$ is

$$(I_t f)(t) = \int_0^t f(s)\, ds. \tag{21}$$

3. TBC for the NNLS equation on metric graphs

Metric graphs, which are the one- or quasi-one-dimensional branched wires, considered as the set of bonds with assigned length and connected at the vertices. The connection rule is called the topology of a graph and is given in terms of the the adjacency matrix [18, 19]:

$$A_{ij} = \begin{cases} 1 & \text{if there is a bond connecting vertex } i \text{ to vertex } j, \\ 0 & \text{otherwise.} \end{cases}$$

The topology of a graph can vary in complexity and accommodate a wide range of structures. However, one of the most fundamental and widely studied graph topologies is the star graph. A star graph consists of a single central vertex from which all links emanate. The star graph can be viewed as the elementary building block for constructing more complex graph topologies. By appropriately connecting multiple star graphs, one can generate a wide variety of graph configurations. This approach motivates the study of transparent vertices on star graphs, which can be extended to other topologies.

3.1. NNLS equation on a star graph

One of the restrictions on the class of initial conditions for NNLS equation is that they must be even (in x), which makes the initial data symmetric with respect to the y-axis. Taking this property into account, we consider the simplest possible star graph with an even number of bonds by denoting its bonds as $b_{\pm j}, j = 1, 2$ (see, figure 1). Coordinates $x_{\pm j}$ are assigned to and the NNLS equation is written for the each bond of the star graph as

$$\mathrm{i}\partial_t q_{\pm j}(x,\, t) + \partial_x^2 q_{\pm j}(x,\, t) + \sqrt{\beta_j \beta_{-j}}\; q_{\pm j}^2(x,\, t) q_{\mp j}^*(-x,\, t) = 0, \tag{22}$$

where $q_{\pm j}(x, t)$ are defined in $x \in b_{\pm j}$, and $j = 1, 2$. We choose the coordinates of bonds b_{-j} as $x_{-j} \in (-\infty, 0)$ and for b_j as $x_j \in [0, +\infty)$, so that the origin of the coordinates falls on the vertex.

The equation (22) represents a system of NNLS equations in which the components $q_{\pm j}$ are mixed in the nonlinear term through the factor $\sqrt{\beta_j \beta_{-j}}$. In order to solve this system, boundary conditions must be set at the branching point (vertex) of the graph. We adopt the boundary conditions established in [38], which ensure the

integrability of the system by demonstrating the existence of infinitely many conservation laws. In this framework for the above NNLSE, the norm is defined as (see [1])

$$N(t) = \sum_{j=1}^{2}[N_j(t) + N_{-j}(t)], \quad N_{\pm j}(t) = \int_{b_{\pm j}} q_{\pm j}(x,\, t) q^{*}_{\mp j}(-x,\, t)\, dx. \tag{23}$$

The energy, being another conserving quantity, is given by

$$\begin{aligned} E(t) &= \sum_{j=1}^{2}[E_j(t) + E_{-j}(t)], \\ &\times E_{\pm j}(t) = \int_{b_{\pm j}} \left(\partial_x q_{\pm j}(x,\, t) \cdot \partial_x q^{*}_{\mp j}(-x,\, t) + \frac{\sqrt{\beta_j \beta_{-j}}}{2} q^{2}_{\pm j}(x,\, t) \cdot q^{*2}_{\mp j}(-x,\, t) \right) dx. \end{aligned} \tag{24}$$

By requiring the conservation of these quantities, the time derivatives of the norm and the energy lead to the following vertex boundary conditions [38]:

$$\begin{aligned} &\gamma_1 q_1(x,\, t)|_{x=0} = \gamma_{-1} q_{-1}(x,\, t)|_{x=0} = \gamma_2 q_2(x,\, t)|_{x=0} = \gamma_{-2} q_{-2}(x,\, t)|_{x=0}, \\ &\frac{1}{\gamma_1}\partial_x q_1(x,\, t)\,\Big|_{x=0} + \frac{1}{\gamma_2}\partial_x q_2(x,\, t)\,\Big|_{x=0} = \frac{1}{\gamma_{-1}}\partial_x q_{-1}(x,\, t)\,\Big|_{x=0} + \frac{1}{\gamma_{-2}}\partial_x q_{-2}(x,\, t)\,\Big|_{x=0}, \end{aligned} \tag{25}$$

where the parameters $\gamma_{\pm j}$ are non-zero positive real numbers.

Then, we express the solution of the problem given by equations (22) and (25) in terms of the solution of equation (1) as

$$q_{\pm j}(x,\, t) = \sqrt{\frac{2}{\beta_{\pm j}}}\, q(x,\, t), \tag{26}$$

and it satisfies the boundary conditions (25), when the following conditions hold:

$$\frac{\gamma_{\pm j}}{\gamma_{-1}} = \sqrt{\frac{\beta_{\pm j}}{\beta_{-1}}}, \qquad \frac{1}{\beta_1} + \frac{1}{\beta_2} = \frac{1}{\beta_{-1}} + \frac{1}{\beta_{-2}}. \tag{27}$$

A traveling soliton solution of equation (3) given on a graph can be written as

$$q_{\pm j}(x,\, t) = \sqrt{\frac{2}{\beta_{\pm j}}}\, \frac{\alpha_1\, e^{-\Delta/2}\, e^{(\bar{\xi}_{1R} - \xi_{1R}) + \mathrm{i}(\bar{\xi}_{1I} - \xi_{1I})}}{2[\cosh(\chi_1)\cos(\chi_2) + \mathrm{i}\sinh(\chi_1)\sin(\chi_2)]}. \tag{28}$$

The sum rule (27) can be considered as a condition (constraint) that ensures the integrability of NNLS equation on a metric star graph given by equations (22) and (25). In other words, if the sum rule (27) is fulfilled, there exist an analytical solution which can be expressed as equation (28).

3.2. Derivation of transparent vertex boundary conditions

In this subsection, we derive the TBC for the NNLS equation on graphs by applying the potential approach used in the derivation of TBCs on a line. Subsequently, the NNLS equation can be formally written as a linear partial differential equation (PDE)

$$\mathrm{i}\partial_t q_{\pm j}(x,\, t) + \partial_x^2 q_{\pm j}(x,\, t) + V_{\pm j}(x,\, t) q_{\pm j}(x,\, t) = 0, \tag{29}$$

where $V_{\pm j}(x,\, t) = \sqrt{\beta_j \beta_{-j}}\; q_{\pm j}(x,\, t) q^{*}_{\mp j}(-x,\, t)$.

We now divide the entire domain (graph) into two subdomains, referred to as the 'interior' (bonds $b_{\pm 1}$) and the 'exterior' (bonds $b_{\pm 2}$). These terms are used to maintain consistency with the terminology adopted for the problem on a line. Moreover, the terminologies are borrowed from the original works [21, 39–41], where the core idea of constructing TBCs was introduced. Accordingly, we proceed by considering both the interior and exterior problems. The interior problem for $b_{\pm 1}$ can be expressed as

$$\begin{aligned} &\mathrm{i}\partial_t q_{\pm 1} + \partial_x^2 q_{\pm 1} + V_{\pm 1}(x,\, t) q_{\pm 1} = 0, \\ &q_{\pm 1}|_{t=0} = Q^{I}(x), \\ &\partial_x q_{\pm 1}|_{x=0} = \pm (T_0 q_{\pm 1})|_{x=0}, \end{aligned} \tag{30}$$

where $Q^{I}(x)$ is an initial condition and T_0 is yet an unknown operator that determines the TBCs.

The exterior problems for $b_{\pm 2}$ reads

$$\begin{aligned} &\mathrm{i}\partial_t q_{\pm 2} + \partial_x^2 q_{\pm 2} + V_{\pm 2}(x,\,t) q_{\pm 2} = 0, \\ &q_{\pm 2}|_{t=0} = 0, \\ &q_{\pm 2}|_{x=0} = \psi_{\pm 2}(t), \quad \psi_{\pm 2}(0) = 0, \\ &(T_0 \psi_{\pm 2})|_{x=0} = \mp \partial_x q_{\pm 2}|_{x=0}. \end{aligned} \tag{31}$$

We introduce a new function

$$\mu_{\pm j}(x,\,t) = e^{-\mathrm{i}\nu_{\pm j}(x,t)} q_{\pm j}(x,\,t), \tag{32}$$

where

$$\nu_{\pm j}(x,\,t) = \int_0^t V_{\pm j}(x,\,\tau)\,d\tau = \sqrt{\beta_j \beta_{-j}} \int_0^t q_{\pm j}(x,\,\tau) q_{\mp j}^*(-x,\,\tau)\,d\tau. \tag{33}$$

Then, the TBCs of the second order approximation (19) for $q_{\pm 2}$ at $x = 0$ can be written as

$$\partial_x q_{\pm 2}|_{x=0} = \pm e^{-\mathrm{i}\frac{\pi}{4}} e^{\mathrm{i}\nu_{\pm 2}} \cdot \partial_t^{1/2}(e^{-\mathrm{i}\nu_{\pm 2}} q_{\pm 2})|_{x=0} \pm \mathrm{i}\frac{1}{4} \partial_x V_{\pm 2} e^{\mathrm{i}\nu_{\pm 2}} I_t(e^{-\mathrm{i}\nu_{\pm 2}} q_{\pm 2})|_{x=0}, \tag{34}$$

where the fractional $1/2$-derivative and I_t are given by (20) and (21), correspondingly.

Thus, we find the T_0 operator for $q_{\pm j}$ for $x = 0$ as

$$(T_0 q_{\pm j})|_{x=0} = -e^{-\mathrm{i}\frac{\pi}{4}} e^{\mathrm{i}\nu_{\pm 2}} \cdot \partial_t^{1/2}(e^{-\mathrm{i}\nu_{\pm j}} q_{\pm j})|_{x=0} - \mathrm{i}\frac{1}{4} \partial_x V_{\pm j} e^{\mathrm{i}\nu_{\pm j}} I_t(e^{-\mathrm{i}\nu_{\pm j}} q_{\pm j}) \Big|_{x=0}. \tag{35}$$

To find the TBC for $q_{\pm 1}$ at $x = 0$, we apply operator T_0 to $q_{\pm 1}$ as

$$\partial_x q_{\pm 1}|_{x=0} = \mp e^{-\mathrm{i}\frac{\pi}{4}} e^{\mathrm{i}\nu_{\pm 2}} \cdot \partial_t^{1/2}(e^{-\mathrm{i}\nu_{\pm 2}} q_{\pm 2})|_{x=0} \mp \mathrm{i}\frac{1}{4} \partial_x V_{\pm 2} e^{\mathrm{i}\nu_{\pm 2}} I_t(e^{-\mathrm{i}\nu_{\pm 2}} q_{\pm 2}) \Big|_{x=0}. \tag{36}$$

From the continuity of the solution in equation (25) we have

$$\begin{aligned} &\nu_{-1}(0,\,t) = \nu_{-2}(0,\,t) = \nu_1(0,\,t) = \nu_2(0,\,t), \\ &V_{-1}(0,\,t) = V_{-2}(0,\,t) = V_1(0,\,t) = V_2(0,\,t), \\ &\sqrt{\beta_{-1}}\,(T_0 q_{-1})|_{x=0} = \sqrt{\beta_1}\,(T_0 q_1)|_{x=0} = \sqrt{\beta_{-2}}\,(T_0 q_{-2})|_{x=0} = \sqrt{\beta_2}\,(T_0 q_2)|_{x=0}. \end{aligned} \tag{37}$$

And the current conservation condition in (25) leads to

$$\frac{1}{\sqrt{\beta_{-1}}}(T_0 q_{-1}) \Big|_{x=0} + \frac{1}{\sqrt{\beta_1}}(T_0 q_1) \Big|_{x=0} = \frac{1}{\sqrt{\beta_{-2}}}(T_0 q_{-2}) \Big|_{x=0} + \frac{1}{\sqrt{\beta_2}}(T_0 q_2) \Big|_{x=0}. \tag{38}$$

Comparing the above equations (37) and (38) gives

$$\frac{1}{\beta_{-1}} + \frac{1}{\beta_1} = \frac{1}{\beta_{-2}} + \frac{1}{\beta_2}. \tag{39}$$

Therefore, satisfying the sum rule (39) ensures that the vertex boundary conditions (25) are equivalent to the TBCs at the graph's vertex. In other words, the vertex becomes 'transparent' with respect to soliton transmission. However, since the solution given by equation (26) describes a traveling soliton, such 'transparency' implies that solitons moving from bonds $b_{\pm 1}$ to bonds $b_{\pm 2}$ transmit through the vertex without any reflection. Such a property can be demonstrated in the numerical experiments presented in the next section. Note that the sum rule (39) is different from the one given by (27) and they coincide only if the parameters $\beta_{\pm j}$ have certain values (for example, if all parameters have the same value, $\beta_{-1} = \beta_1 = \beta_{-2} = \beta_2$, which implies natural boundary conditions). This implies that unlike to the case of classical NLS equation [20, 23], for NNLS equation on metric graphs, integrability is not equivalent to the 'transparency' of the vertex.

4. Numerical experiment

Here we show the results of a numerical experiment performed to verify the results of deriving transparent vertex boundary conditions for the NNLS equation on the star graph shown in figure 1. In this numerical experiment we use Runge-Kutta method. In all examples we will use the following initial setup: the initial conditions are imposed on b_{-1} and b_1 symmetric bonds and chosen as analytical solutions in equation (28), where its parameters are given as $\alpha_1 = 1.13 + 1.13\mathrm{i}$, $\beta_1 = 1.13 - 1.13\mathrm{i}$ (should not be confused with boundary conditions parameters) and $k_1 = \pm 2.5 + 1.5\mathrm{i}$, $\bar{k}_1 = \mp 2.5 + 1.5\mathrm{i}$ for $b_{\pm 1}$ bonds, respectively.

As a first example we consider the case, when the sum rule (27) is satisfied. The evolution of the traveling solitons for this case is shown in figure 2 in four consecutive time steps. The figure shows that even when the sum

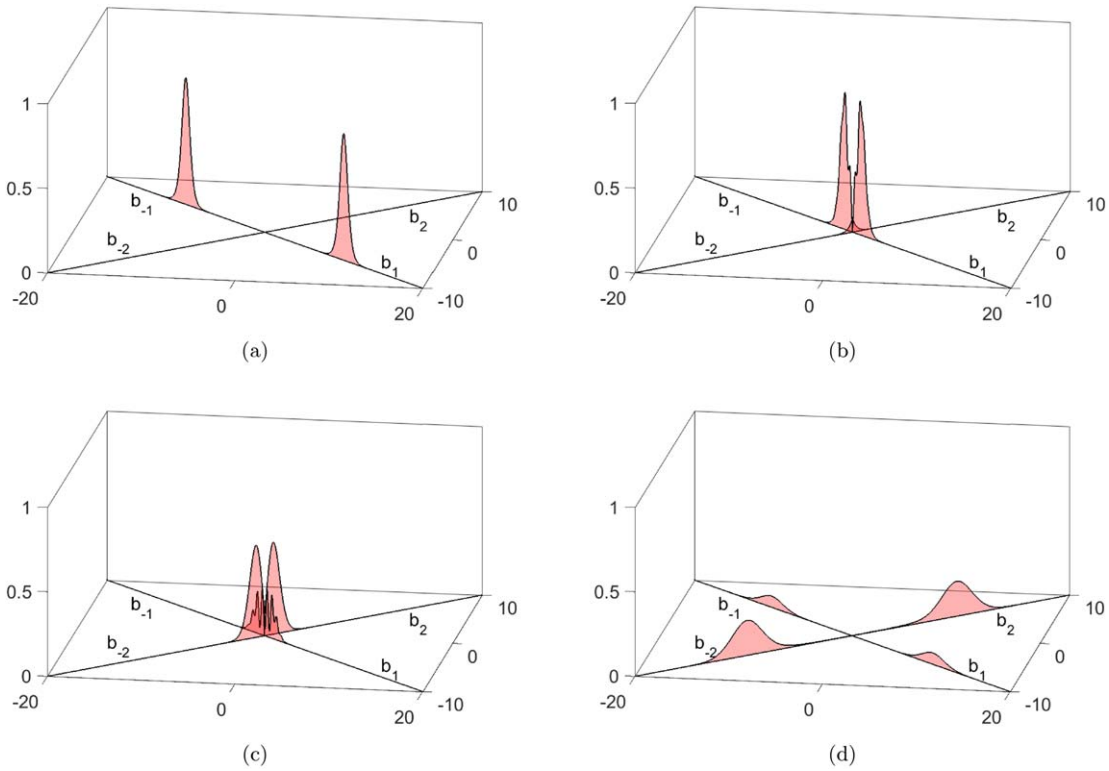

Figure 2. Soliton dynamics at different time moments, i.e., $t = 0$ (a), $t = 0.9$ (b), $t = 1.1$ (c) and $t = 2$ (d) when the sum rule in equation (27) is fulfilled by choosing the following values of the nonlinearity coefficients: $\beta_{\pm 1} = 6$ and $\beta_{\pm 2} = 2$.

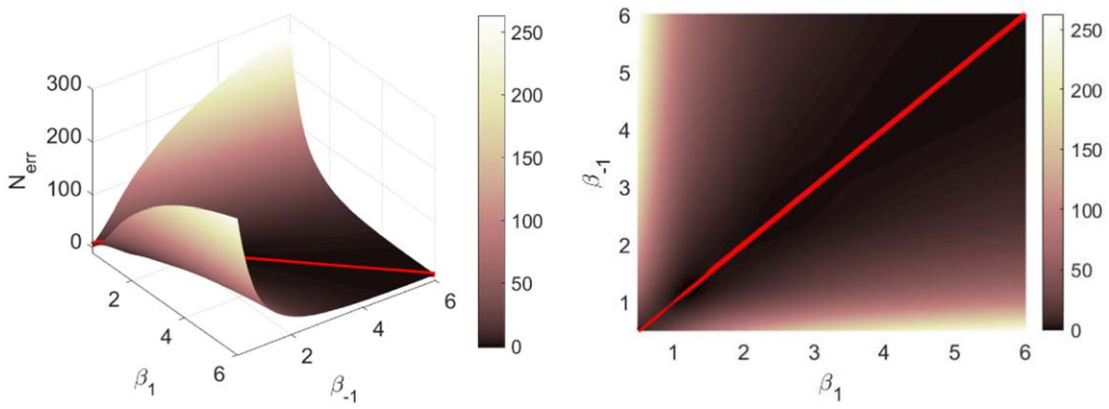

Figure 3. Dependence of the norm conservation on values of parameter β_{-1} and β_1 for fixed $\beta_{-2} = \beta_2 = 2$.

rule in equation (27) is satisfied, a reflection from the vertex of the graph is still clearly observed. This means that the sum rule (27) does not ensure the transparency of the vertex. This example can be supported by determining the set of parameters pairs (β_{-1}, β_1) for some fixed $\beta_{-2} = \beta_2$. Figure 3 shows the dependence of the deviation of the norm from its mean as a function of the parameters (β_{-1}, β_1). In this figure you can see the conservation of the norm along the red line, which confirms the satisfaction of the sum rule (27) derived from the conservation laws, i.e. $\beta_{-1} = \beta_1$. The deviation of the norm from its mean over the whole time is defined as

$$N_{\text{err}} = \int_0^T |\bar{N} - N|\, dt, \tag{40}$$

where

$$\bar{N} = \frac{1}{T}\int_0^T N(t)\, dt$$

is the average value of the total norm over the whole time and T is the total traveling time.

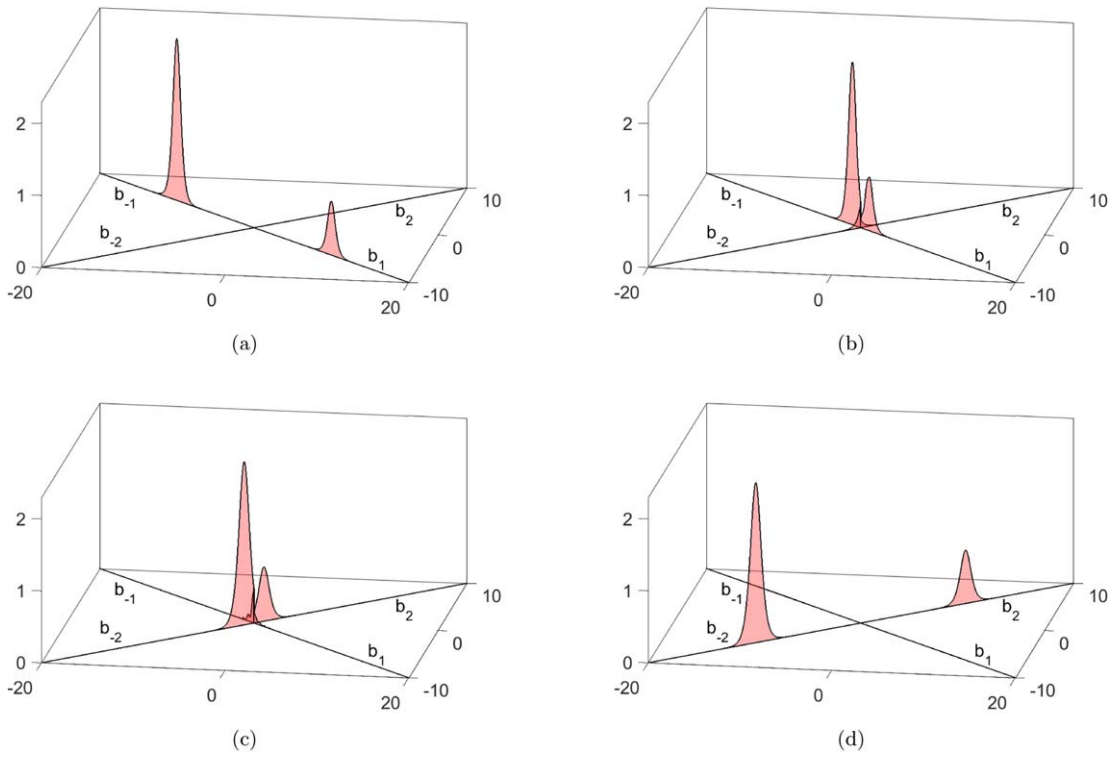

Figure 4. Soliton dynamics at different time moments, i.e., $t = 0$ (a), $t = 0.9$ (b), $t = 1.1$ (c) and $t = 2$ (d) when the sum rule in equation (39) is fulfilled by choosing the following values of the nonlinearity coefficients: $\beta_{-1} = \beta_{-2} = 2$ and $\beta_1 = \beta_2 = 6$.

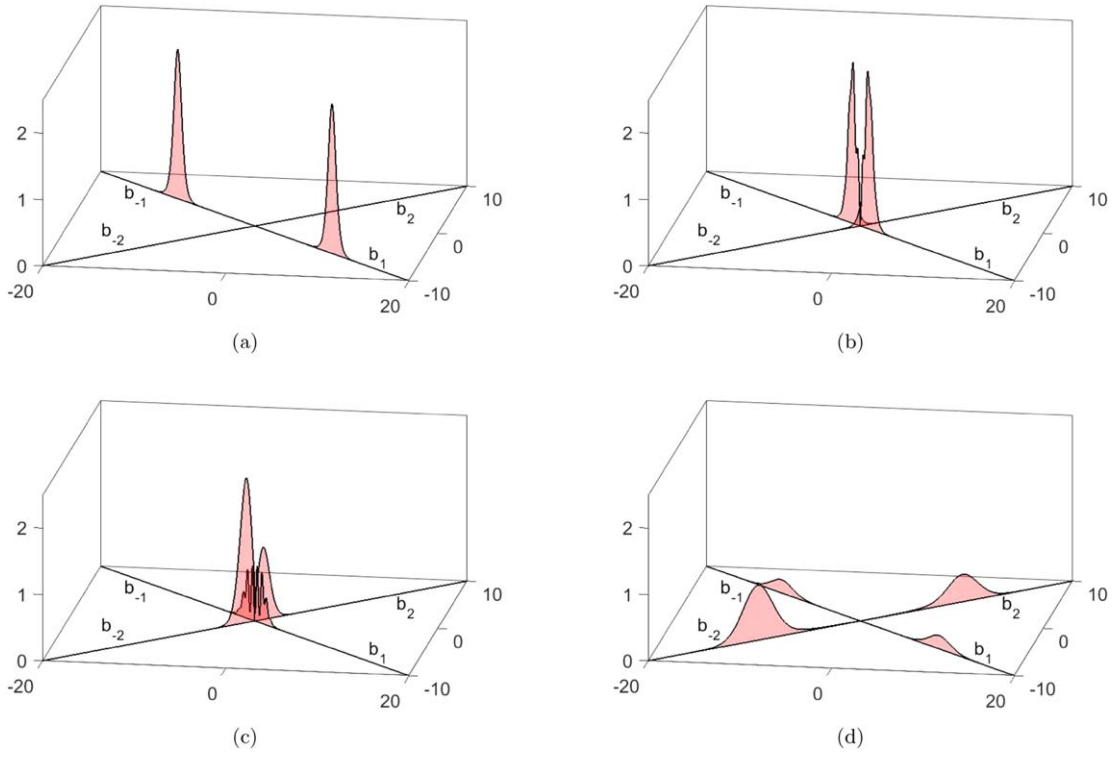

Figure 5. Soliton dynamics at different time moments, i.e., $t = 0$ (a), $t = 0.9$ (b), $t = 1.1$ (c) and $t = 2$ (d) when the sum rules in equations (27) and (39) are broken by choosing the following values of the nonlinearity coefficients: $\beta_{-1} = \beta_1 = 2$ and $\beta_{-2} = 0.5$, $\beta_2 = 1$.

The second example considers the case where the sum rule (39) is satisfied, meaning that TBCs are applied at the central vertex. Figure 4 shows the evolution of the traveling solitons for this case in four consecutive time steps. The reflectionless transmission of the solitons is evident from this plot. It shows the transparency of the

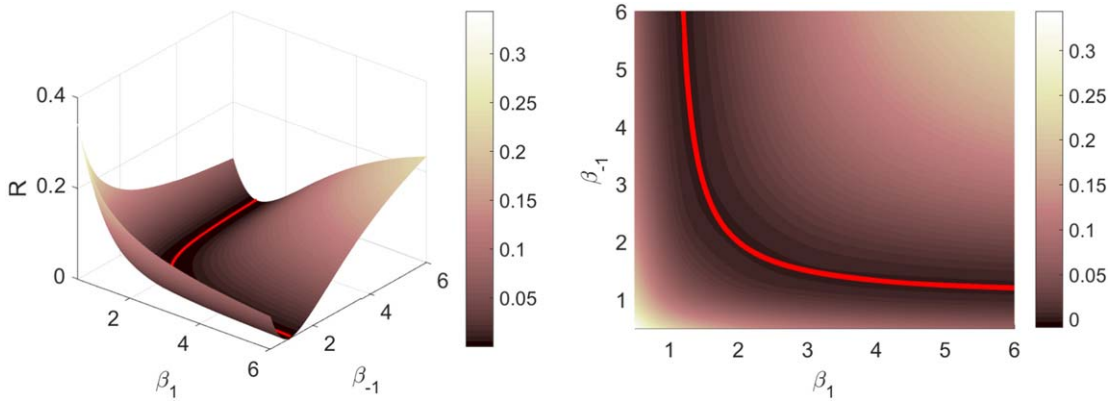

Figure 6. Dependence of the reflection coefficient on values of parameter β_{-1} and β_1 for fixed $\beta_{-2} = \beta_2 = 2$.

vertex of the graph, which is achieved by choosing certain values of the nonlinearity coefficients $\beta_{\pm j}$ that lie on the red line in figure 6 (explained below). As the last example, we consider the case where both sum rules (27) and (39) are violated. The results of the calculations are shown in figure 5. In this plot one can observe the reflection at the vertex of the graph. Furthermore, the NNLS equation is no longer integrable due to violation of the constraint (27).

Note that the choice of parameters (β_{-1}, β_1) is obviously not unique for some fixed β_{-2} and β_2. This can be verified by plotting the dependence of the reflection coefficient on the parameters (β_{-1}, β_1). For some fixed time instant t_0, the reflection coefficient can be defined as

$$R = \frac{N_{-1} + N_1}{N_{-1} + N_1 + N_{-2} + N_2}, \tag{41}$$

where $N_{\pm j}$ are partial norms in equation (23) of bonds $b_{\pm j}$ at time t_0. The plot of the reflection coefficient as a function of the BC parameters (β_{-1}, β_1) for fixed $\beta_{-2} = \beta_2 = 2$ at sufficient time $(t = 2)$ is shown in figure 6. From this plot one can see the black curve (highlighted by the red line) bounded by the values of the parameters (β_{-1}, β_1) that satisfy the equation $\beta_{-1}^{-1} + \beta_1^{-1} = 1$. This shows the manifestation of the reflectionless transition of solitons when the constraint (39) is satisfied.

5. Conclusions

In this paper, we studied the reflectionless transport of solitons governed by the PT-symmetric nonlocal nonlinear Schrödinger equation on metric graphs. Using the so-called potential approach, we derived transparent boundary conditions imposed at the vertices. We identified conditions under which transparent boundary conditions are equivalent to weight-continuity and generalized Kirchhoff conditions. Numerical utilization of transparent boundary conditions and numerical proof of their equivalence to weight-continuity and generalized Kirchhoff rules are provided. For PT-symmetric solitons, the transparency implies the reflectionless transmission of a 'wing' of the soliton from the bond $b_{\pm 1}$ to the bond $b_{\pm 2}$. The results obtained in this work can be applied to the modeling of optical networks and optoelectronic devices using PT-symmetric solitons, so that the minimum signal loss can be achieved by tuning the soliton propagation.

Acknowledgments

The work is supported by the grants of the Agency for innovative development under the Ministry of higher education, science and innovation of the Republic of Uzbekistan (Ref. No. F-2021-440 and FZ-5821512021).

Data availability statement

No new data were created or analysed in this study.

ORCID iDs

M E Akramov
J R Yusupov https://orcid.org/0000-0003-1758-6805
M Ehrhardt https://orcid.org/0000-0003-2561-8854
H Susanto https://orcid.org/0000-0003-0425-107X
D U Matrasulov https://orcid.org/0000-0001-8957-0058

References

[1] Ablowitz M J and Musslimani Z H 2013 Integrable nonlocal nonlinear Schrödinger equation *Phys. Rev. Lett.* **110** 064105
[2] Ablowitz M J and Musslimani Z H 2014 Integrable discrete *PT* symmetric model *Phys. Rev.* E **90** 032912
[3] Ablowitz M J and Musslimani Z H 2016 Inverse scattering transform for the integrable nonlocal nonlinear Schrödinger equation *Nonlinearity* **29** 915
[4] Ablowitz M J and Musslimani Z H Integrable nonlocal nonlinear equations *Stud. Appl. Math.* **139** 7
[5] Feng B-F, Luo X-D, Ablowitz M J and Musslimani Z H 2018 General soliton solution to a nonlocal nonlinear Schrödinger equation with zero and nonzero boundary conditions *Nonlinearity* **31** 5385
[6] Ablowitz M J, Luo X-D and Musslimani Z H 2018 Inverse scattering transform for the nonlocal nonlinear Schrödinger equation with nonzero boundary conditions *J. Math. Phys.* **59** 011501
[7] Ablowitz M J and Musslimani Z H 2019 Integrable nonlocal asymptotic reductions of physically significant nonlinear equations *J. Phys.* A **52** 15LT02
[8] Stalin S, Senthilvelan M and Lakshmanan M 2017 Nonstandard bilinearization of *PT*-invariant nonlocal nonlinear Schrödinger equation: bright soliton solutions *Phys. Lett.* A **381** 2380
[9] Wen Z and Zh Y 2017 Solitons and their stability in the nonlocal nonlinear Schrödinger equation with *PT*-symmetric potentials *Chaos* **27** 053105
[10] Yang J 2018 Physically significant nonlocal nonlinear Schrödinger equation and its soliton solutions *Phys. Rev.* E **98** 042202
[11] Sinha D and Ghosh P K 2015 Symmetries and exact solutions of a class of nonlocal nonlinear Schrödinger equations with self-induced parity-time-symmetric potential *Phys. Rev.* E **91** 042908
[12] Rusin R, Kusdiantara R and Susanto H 2019 Variational approximations of soliton dynamics in the Ablowitz-Musslimani nonlinear Schrödinger equation *Phys. Lett.* A **383** 2039
[13] Wen Z and Yan Z 2019 The nonlinear Schrödinger equation with generalized nonlinearities and *PT*-symmetric potentials: stable solitons, interactions, and excitations *Phys. Lett.* A **27** 053105
[14] Maor O, Dror N and Malomed B A 2013 Holding spatial solitons in a pumped cavity with the help of nonlinear potentials *Opt. Lett.* **38** 5454–7
[15] Li J, Zh-J Y and Sh-M Z 2023 Periodic collision theory of multiple cosine-Hermite-Gaussian solitons in Schrödinger equation with nonlocal nonlinearity *Appl. Math. Lett.* **140** 108588
[16] Li J, Zh-P D and Zh-J Y 2024 Periodic transmission theory of circularly symmetric multi-ring solitons in nonlinear Schrödinger equation *Appl. Math. Lett.* **152** 109034
[17] Zh-Y S, Deng D, Zh-G P and Zh-J Y 2024 Nonlinear transmission dynamics of mutual transformation between array modes and hollow modes in elliptical sine-Gaussian cross-phase beams Chaos *Solitons & Fractals* **178** 114398
[18] Kottos T and Smilansky U 1999 Periodic orbit theory and spectral statistics for quantum graphs *Ann. Phys., NY* **274** 76–124
[19] Gnutzmann S and Smilansky U 2006 Quantum graphs: applications to quantum chaos and universal spectral statistics *Adv. Phys.* **55** 527–625
[20] Yusupov J R, Sabirov K K, Ehrhardt M and Matrasulov D U 2019 Transparent nonlinear networks *Phys. Rev.* E **100** 032204
[21] Antoine X, Arnold A, Besse C, Ehrhardt M and Schädle A 2008 A review of transparent and artificial boundary conditions techniques for linear and nonlinear Schrödinger equations *Commun. Comput. Phys.* **4** 729
[22] Adami R, Cacciapuoti C, Finco D and Noja D 2011 Fast solitons on star graphs *Rev. Math. Phys.* **23** 4
[23] Sobirov Z, Matrasulov D, Sabirov K, Sawada S and Nakamura K 2010 Integrable nonlinear Schrödinger equation on simple networks: connection formula at vertices *Phys. Rev.* E **81** 066602
[24] Noja D 2014 Nonlinear Schrödinger equation on graphs: recent results and open problems *Philos. Trans. R. Soc.* A **372** 20130002
[25] Noja D, Pelinovsky D and Shaikhova G 2015 Bifurcations and stability of standing waves in the nonlinear Schrödinger equation on the tadpole graph *Nonlinearity* **28** 2343
[26] Adami R, Cacciapuoti C and Noja D 2016 Stable standing waves for a NLS on star graphs as local minimizers of the constrained energy *J. Diff. Eq.* **260** 7397
[27] Caudrelier V 2015 On the Inverse scattering method for integrable PDEs on a star graph *Comm. Math. Phys.* **338** 893
[28] Adami R, Serra E and Tilli P 2017 Negative energy ground states for the L^2-critical NLSE on metric graphs 2017 *Commun. Math. Phys.* **352** 387
[29] Kairzhan A and Pelinovsky D E 2018 Spectral stability of shifted states on star graphs *J. Phys. A: Math. Theor.* **51** 095203
[30] Yusupov J R, Matyokubov K S, Sabirov K K and Matrasulov D U 2020 Exciton dynamics in branched conducting polymers: quantum graphs based approach *Chem. Phys.* **537** 110861
[31] Matrasulov D, Sabirov K, Babajanov D and Susanto H 2020 Branched Josephson junctions: current carrying solitons in external magnetic fields *EPL* **130** 67002
[32] Sabirov K K, Akramov M E, Otajonov R S and Matrasulov D U 2020 Soliton generation in optical fiber networks *Chaos, Solitons Fractals* **133** 109636
[33] Akramov M E, Yusupov J R, Ehrhardt M, Susanto H and Matrasulov D U 2023 Transparent boundary conditions for the nonlocal nonlinear Schrödinger equation: a model for reflectionless propagation of PT-symmetric solitons *Phys. Lett.* A **459** 128611
[34] Antoine X, Ch B and Descombes S 2006 Artificial boundary conditions for one-dimensional cubic nonlinear Schrödinger equations *SIAM J. Numer. Anal.* **43** 2272
[35] Sabirov K K, Yusupov J R, Aripov M M, Ehrhardt M and Matrasulov D U 2021 Reflectionless propagation of Manakov solitons on a line: a model based on the concept of transparent boundary conditions *Phys. Rev.* E **103** 043305

[36] Sabirov K K, Yusupov J R, Ehrhardt M and Matrasulov D U 2021 Transparent boundary conditions for the sine-Gordon equation: modeling the reflectionless propagation of kink solitons on a line *Phys, Lett.* A **423** 127822
[37] Taylor M 2006 *Pseudo Differential Operators* (Pub. Springer)
[38] Akramov M, Sabirov K, Matrasulov D, Susanto H, Usanov S and Karpova O 2022 Nonlocal nonlinear Schrödinger equation on metric graphs: a model for generation and transport of parity-time-symmetric nonlocal solitons in networks *Phys. Rev.* E **105** 054205
[39] Ehrhardt M 1999 Discrete transparent boundary conditions for general Schrödinger-type equations *VLSI Des.* **9** 325
[40] Ehrhardt M and Arnold A 2001 Discrete transparent boundary conditions for the Schrödinger equation *Riv. di Math. Univ. di Parma* **6** 57
[41] Arnold A, Ehrhardt M and Sofronov I 2003 Discrete transparent boundary conditions for the Schrödinger equation: fast calculation, approximation, and stability *Commun. Math. Sci.* **1** 501